J1 CrIS SDR Algorithm and Software

Yong Han and Yong Chen

Acknowledgement: CrIS SDR science team for the development and improvement of J1 CrIS SDR algorithm

STAR JPSS Science Team Annual Meeting, August 24-28, 2015

Outline

- J1 CrIS SDR baseline algorithm/software
- Proposed J1 CrIS SDR algorithm/software updates
- Summary and future work

Baseline J1 CrIS SDR Algorithm/Software

J1 Baseline Algorithm/Software

- Delivered on January 30, 2015
- New FCE module delivered on May 30, 2015
- Software/software changes
  - Capable to process both normal and full spectral resolution SDRs
  - Backward compatibility (multiple calibration algorithms implemented)
  - CMO file separated into two files: 1) SA-1 matrix; 2) backup of Engineering packet
  - Resampling matrix calculation following neon calibration
  - Resampling and self-apodization matrix algorithms are modified to reduce spectral ringing artifacts
  - Spectral calibration (CMO) applied to radiance noise (NEdN) calculation
  - New FCE detection/correction module

SDR Processing Flow

JPSS-1:

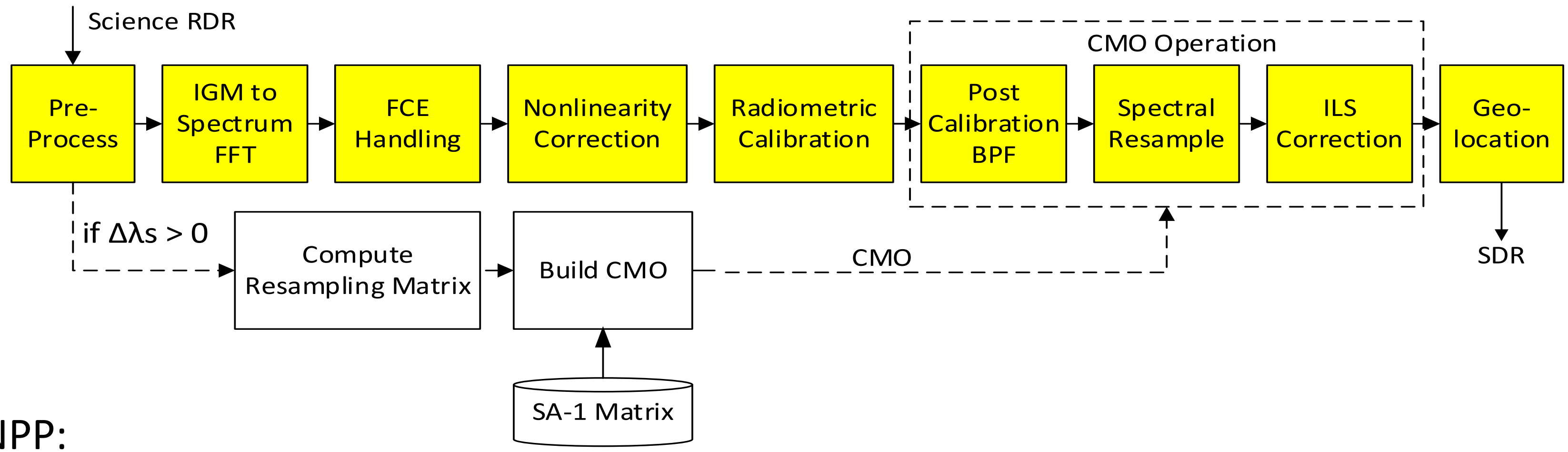

S-NPP:

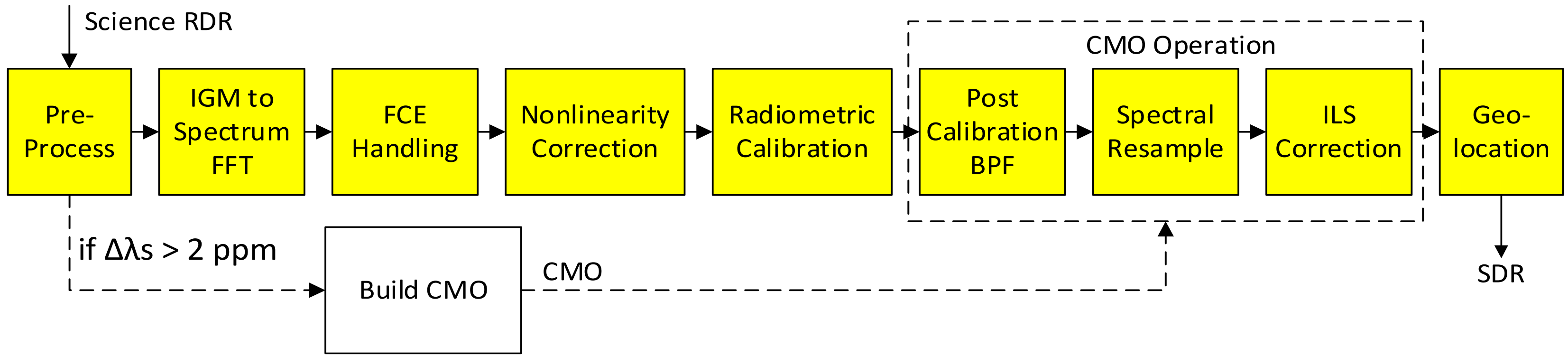

Resampling Algorithm (1/2)

JPSS-1: resampling is performed on un-decimated spectral domain (large N) and the matrix calculation is updated with Mooney's equation:

$$F[k,k'] = \frac{\Delta\sigma_s}{\Delta\sigma_u} \frac{Sin(\pi \frac{\sigma_{s,k'} - \sigma_{u,k}}{\Delta\sigma_u})}{NSin(\pi \frac{\sigma_{s,k'} - \sigma_{u,k}}{N\Delta\sigma_u})}$$

Mooney, 2014

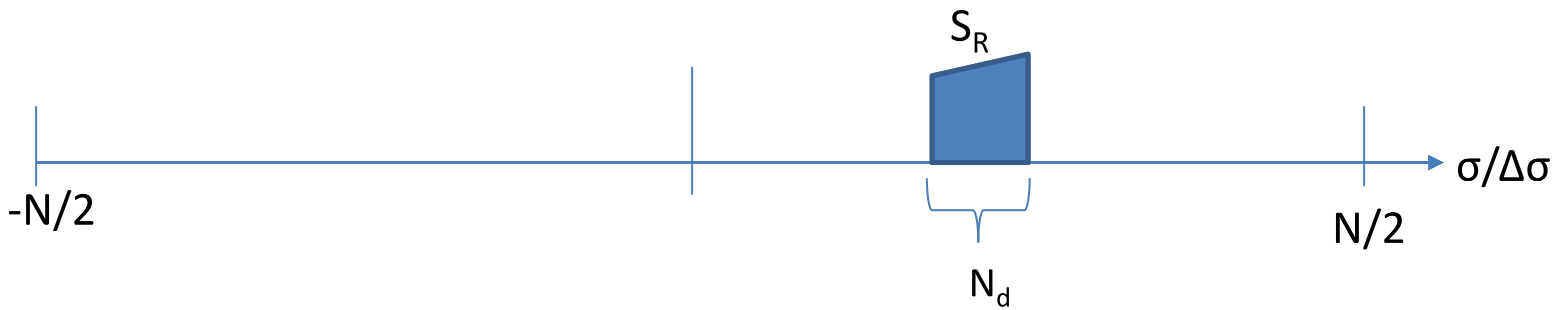

S-NPP: small N and the Eq has a minor error:

$$F[k,k'] = \frac{Sin(\pi \frac{\sigma_{s,k'} - \sigma_{u,k}}{\Delta\sigma_u})}{N_d Sin(\pi \frac{\sigma_{s,k'} - \sigma_{u,k}}{N_d \Delta\sigma_s})}$$

Resampling Algorithm (2/2)

- Big N is used in the J1 delivery; the J1 resampling algorithm is consistent with the Double-FFT method (see backup slides)

JPSS-1:

$$S_{k'} = \frac{\Delta\sigma_s}{\Delta\sigma_u}\sum_{k=0}^{N_d-1} S_k \frac{Sin(\pi\frac{\sigma_{s,k'}-\sigma_{u,k}}{\Delta\sigma_u})}{NSin(\pi\frac{\sigma_{s,k'}-\sigma_{u,k}}{N\Delta\sigma_u})}$$

S-NPP:

$$S_{k'} = \sum_{k=0}^{N_d-1} S_k \frac{1}{N_d}\frac{Sin(\pi\frac{\sigma_{s,k'}-\sigma_{u,k}}{\Delta\sigma_u})}{Sin(\pi\frac{\sigma_{s,k'}-\sigma_{u,k}}{N_d\Delta\sigma_s})}$$

Comparison of using big N and small N (simulated results)

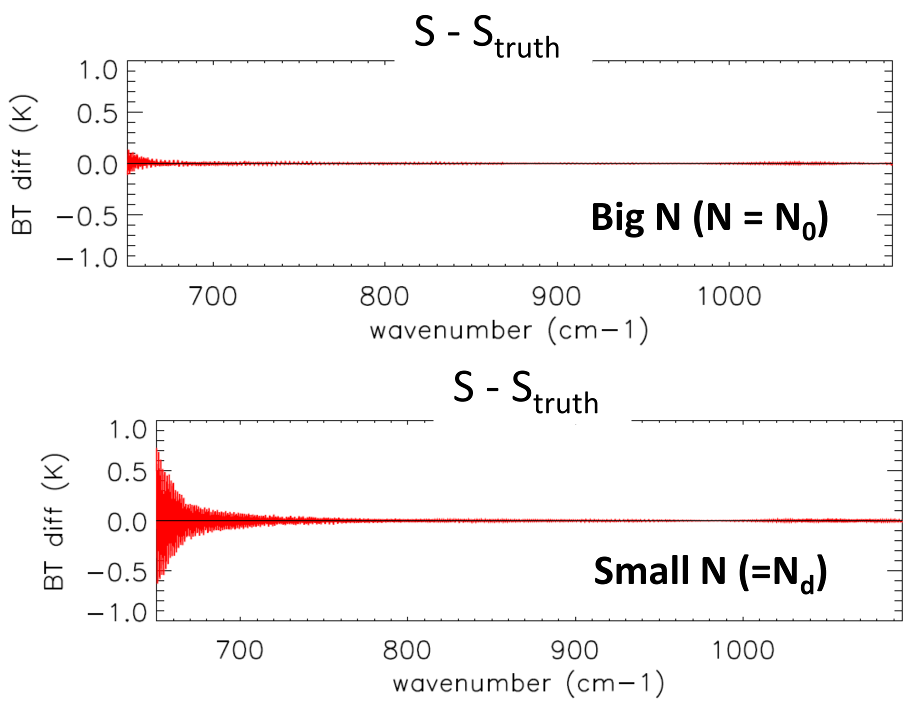

N_d = 866 (LW), 1052 (MW), 799 (SW)

N = 20784 (LW), 21040 (MW), 20744 (SW)

SA Correction Matrix Algorithm (1/2)

Expansion factor β:

- **JPSS-1: 1.4 (LW), 2 (MW), 2 (SW)**
- **SNPP: 1.1, (LW, MW, SW)**

- Big N is used, consistent with the resampling algorithm
- Results of using big N and small N differ little

$$SA[k',k] = \int_{\alpha_{\min}}^{\alpha_{\max}} \text{psinc}((k_0 + k') - \alpha(k_0 + k), N) ILS(\alpha) d\alpha$$

$$\sum_{k'=k0}^{k_0+\beta N_d - 1} SA[k',k] \approx 1$$

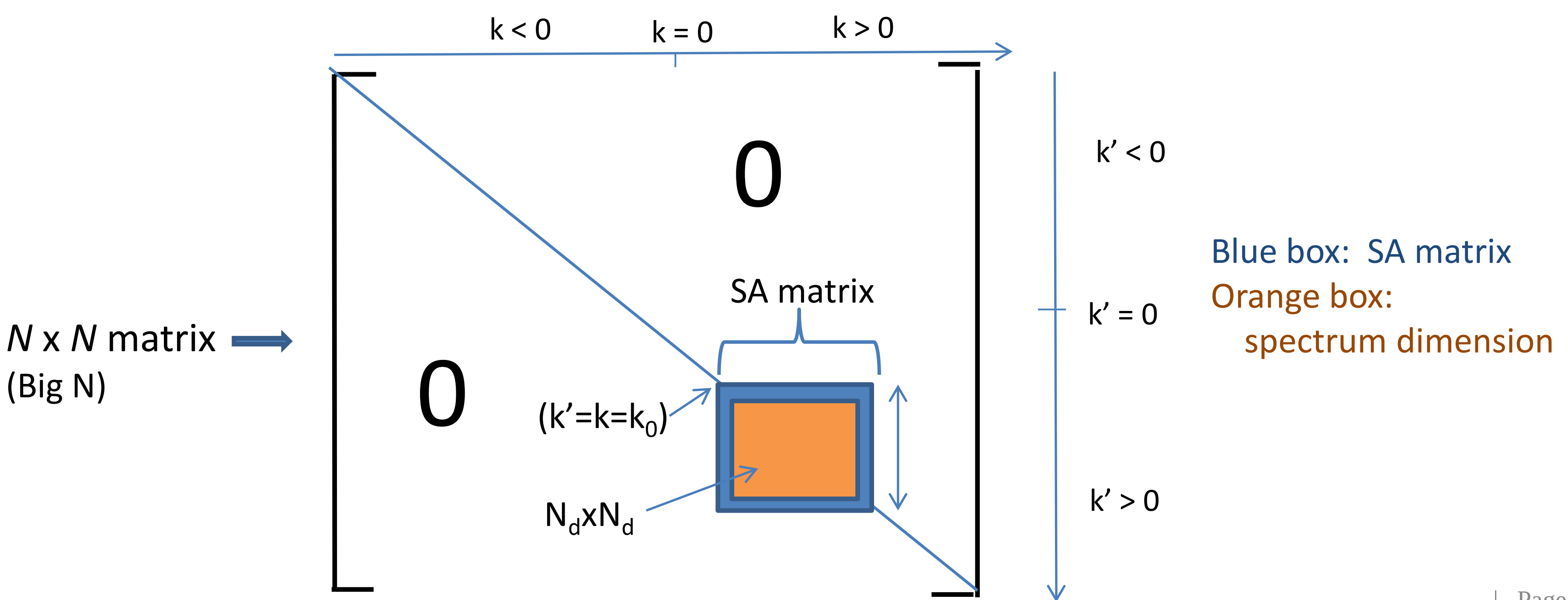

SA Correction Matrix Algorithm (2/2)

The self-apodization (SA) matrix expansion factor is increased from 1.1 to 2.0 for the SW bands to reduce ringing artifacts

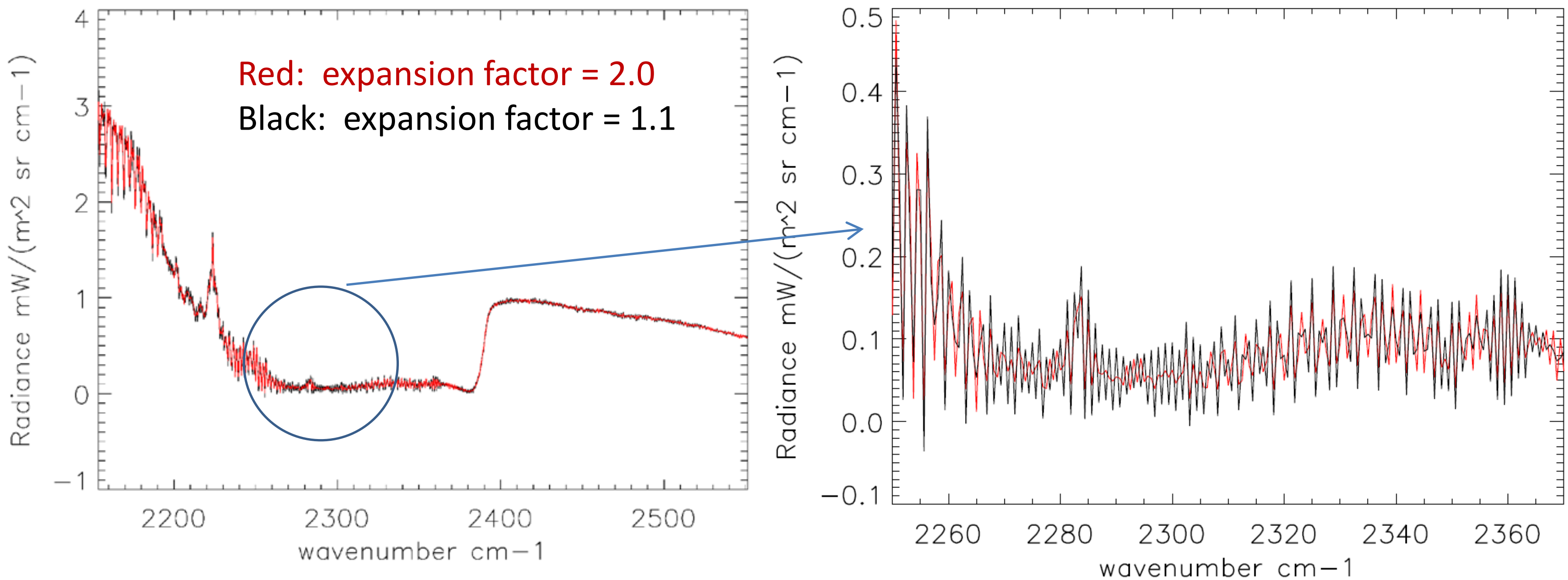

NEdN Algorithm

JPSS-1: CMO applied to NEdN calculation

S-NPP: no CMO applied to NEdN calculation

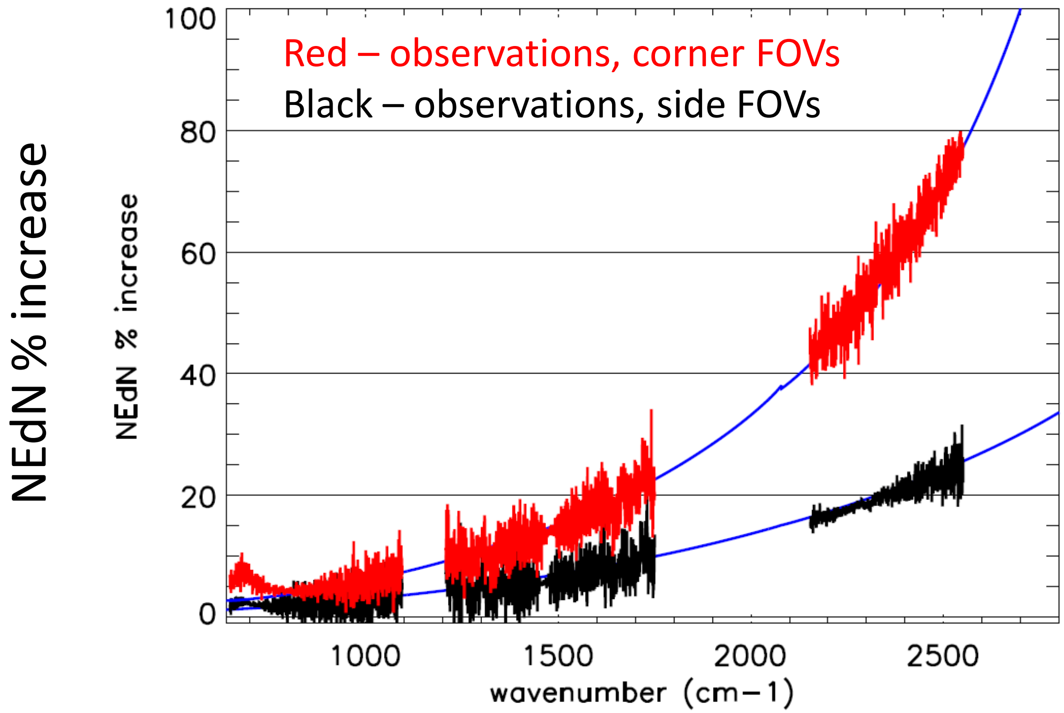

For FSR SDR processing, NEdNs in MW and SW bands are significantly increased by self-apodization (SA) correction

Proposed J1 CrIS SDR Algorithm/Software Updates

Summary of Proposed Updates

- All the updates described in the following slides have already been implemented in the ADL code
- Software/algorithm updates
  - Use of full interferogram data points (reducing ringing artifacts)
  - Raised-cosine post-filter and adjustable filter parameters (reducing ringing artifacts)
  - Algorithm 4 and UMBC CCAST calibration (reducing ringing artifacts)
  - Band-dependent lunar intrusion thresholds added to the PCT file (improving lunar intrusion detection)
  - Sign change for the cross-track offset angles to remove the reordering of the FOV positions in geolocation calculation (?)

Extending Interferogram (1/4)

- Non-circular FIR filtering is an issue which was first brought out by Dan Mooney
- UW demonstrated that it is a root-cause of the ringing artifacts
- UW proposed the following solution to reduce the ringing artifacts (presented on 12 March 2014 team telecon):

(1) Divide out the ideal filter:
FFT(NF*DM)/FFT(NF)

(2) Transform back to the time domain by zero-padding to reconstruct a good approximation to the original DM IFG

(3) Truncate the reconstructed IFG by an amount equivalent to about 5 decimated points

(4) FFT the truncated reconstructed IFG to the spectrum

DM – diagnostic mode interferogram (IFG)
NF – FIR filter
NF*DM – non-circular convolution

Raw spectrum difference from truth

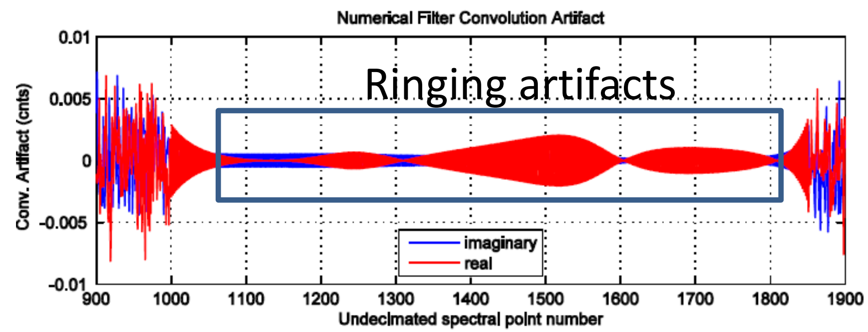

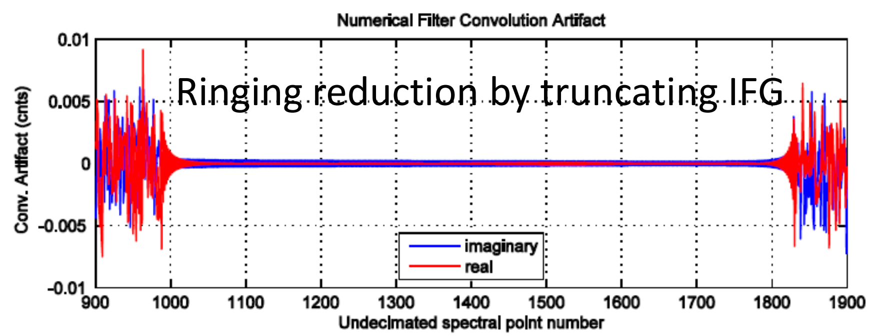

UW

Extending Interferogram (2/4)

- STAR demonstrated that the UW method can be implemented in the spectral domain with the big N resampling matrix *F* (see backup slides):

$$S = F \cdot (S_{raw} / FIR)$$

$$F[k',k] = \frac{\Delta\sigma_s}{\Delta\sigma_u} \frac{Sin(\pi \frac{\sigma_{s,k'} - \sigma_{u,k}}{\Delta\sigma_u})}{N_{big} Sin(\pi \frac{\sigma_{s,k'} - \sigma_{u,k}}{N_{big}\Delta\sigma_u})}$$

Performed in spectral domain:

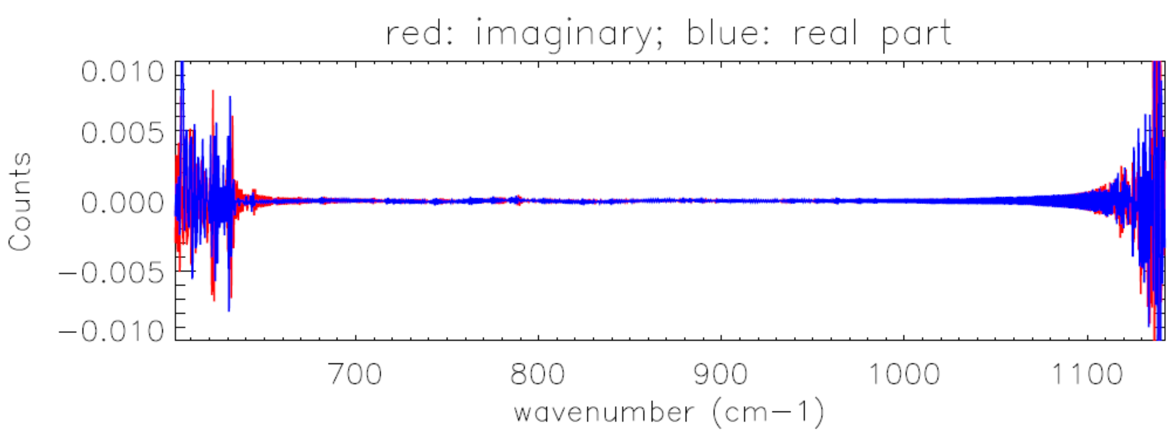

Extending Interferogram (3/4)

- We need 5 or more additional decimated data points beyond MPD for ringing reduction
- In the following we demonstrate even using the two data points currently dropped off by the SDR algorithm can significantly reduces the ringing artifacts:

	LW	MW	SW
Data points used in J1 baseline codes	864	1050	797
Available data points N_d	866	1052	799
N_d*DF	20784	21040	20774
Un-decimated points beyond MPD (λ = 1546.23D-7 cm)	**88**	**344**	**78**

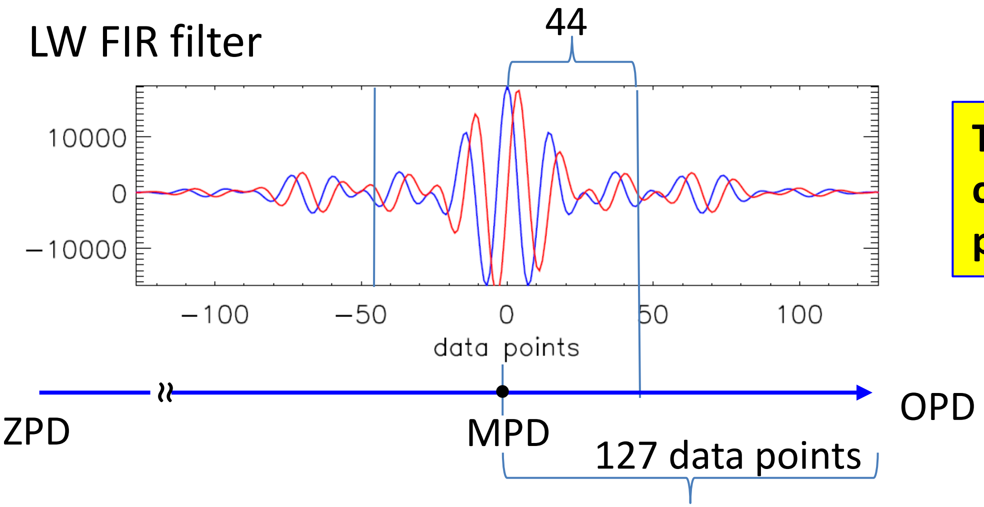

The extended 44 undecimated data points comprise the core of the needed 127 data points beyond the MPD

Extending Interferogram (4/4)

- **Use of the two extra data points significantly reduces the ringing artifacts caused by the non-circular FIR filtering**

Sweep direction difference (FOV-5)

Difference from truth (FOV-1)

N_d = 864

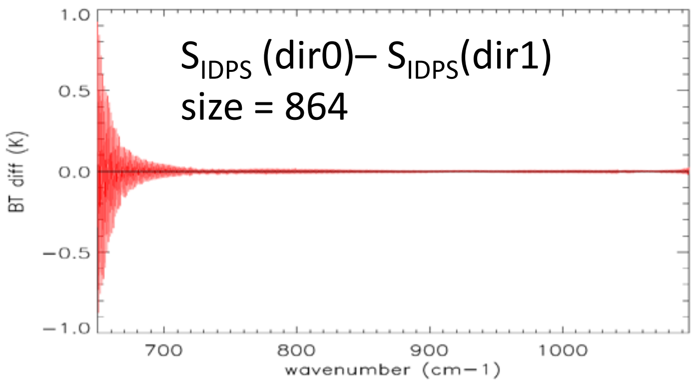

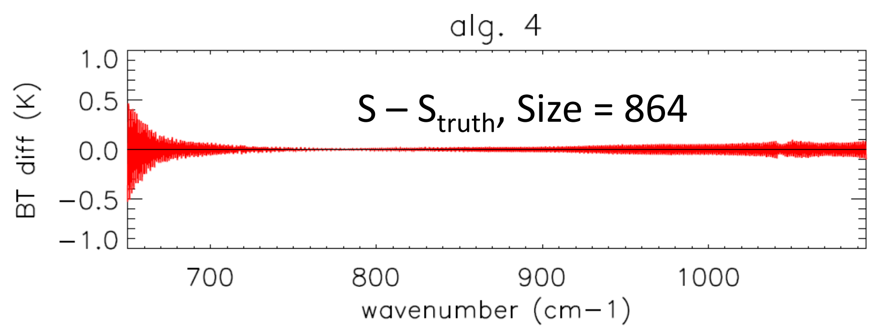

N_d = 866

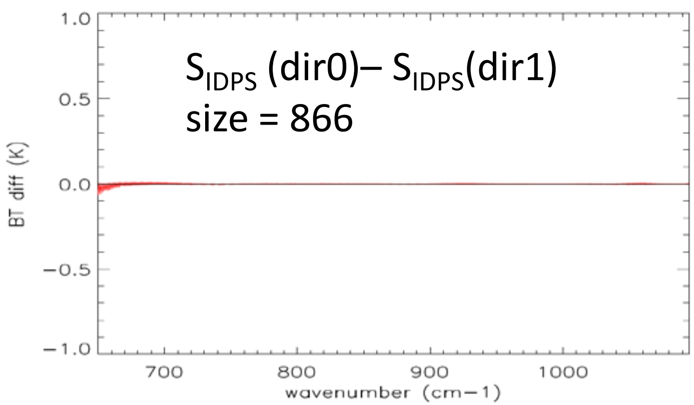

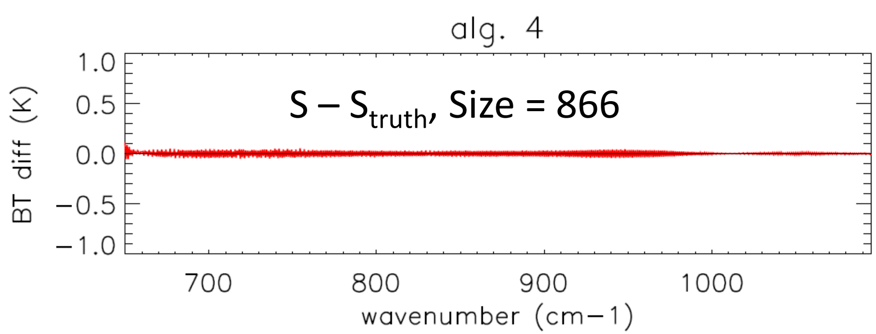

Simulated results

Extending BPF Width (1/2)

Post-filter parameters:

Black – proposed improvement Red – baseline J1 code

	k0	k1	a1	a2	a3	a4
LW	78	790	30 (15)	0.5	30 (15)	0.5
MW	95	959	59 (44)	0.5	59 (44)	0.5
SW	84	716	41 (32)	0.5	41 (32)	0.5

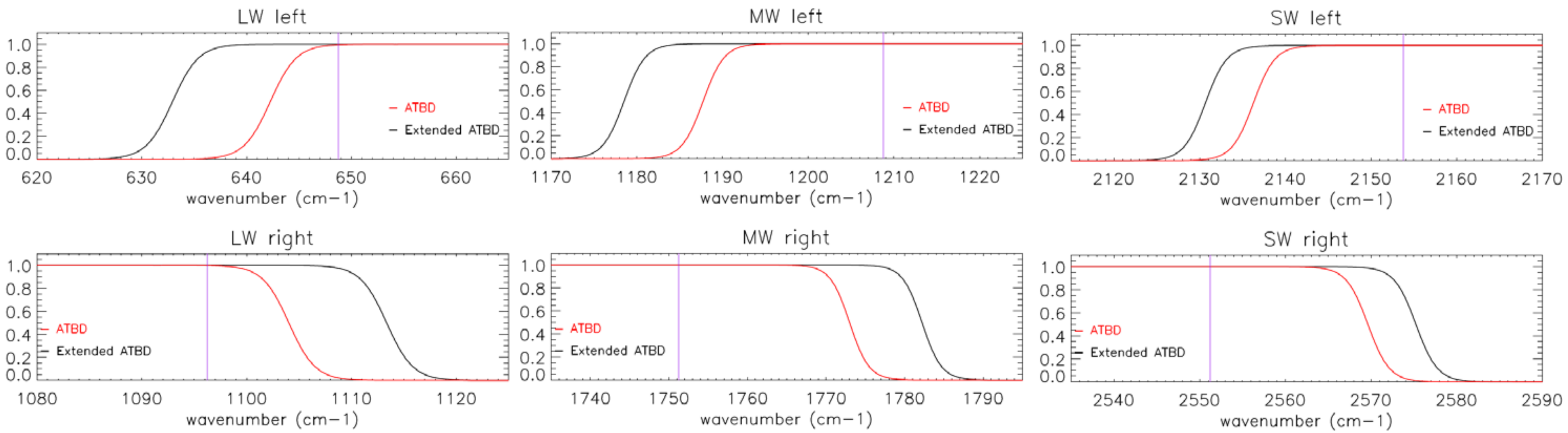

Use of a wider PF preserves useful information for edge channels

Extending BPF Width (2/2)

- Use of a wider PF preserves useful information for edge channels

Narrow Post-filter (FOV-5)

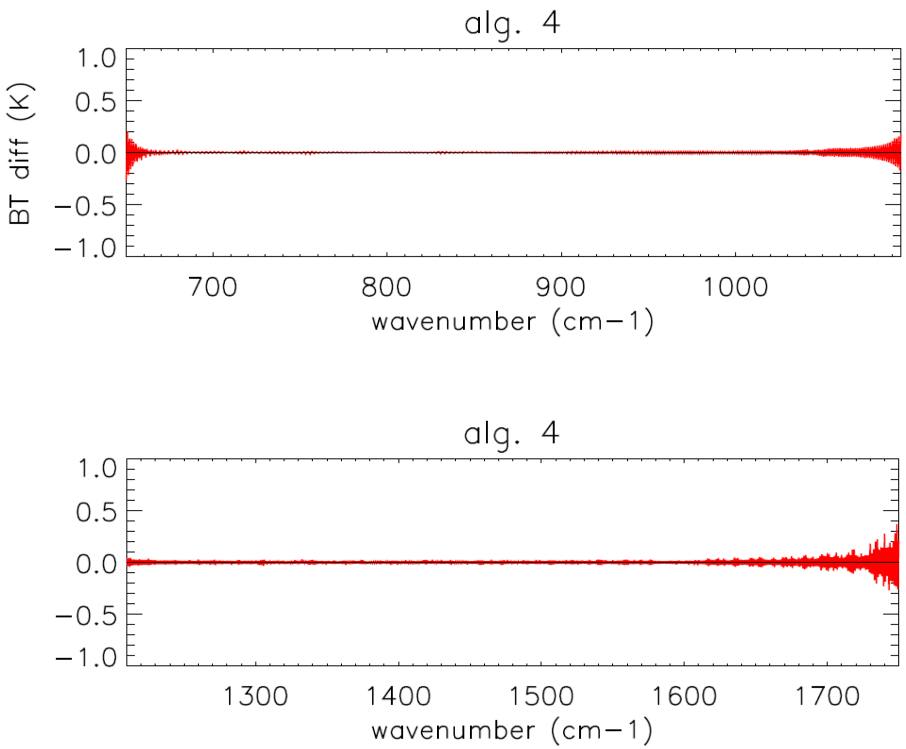

Wide Post-filter (FOV-5)

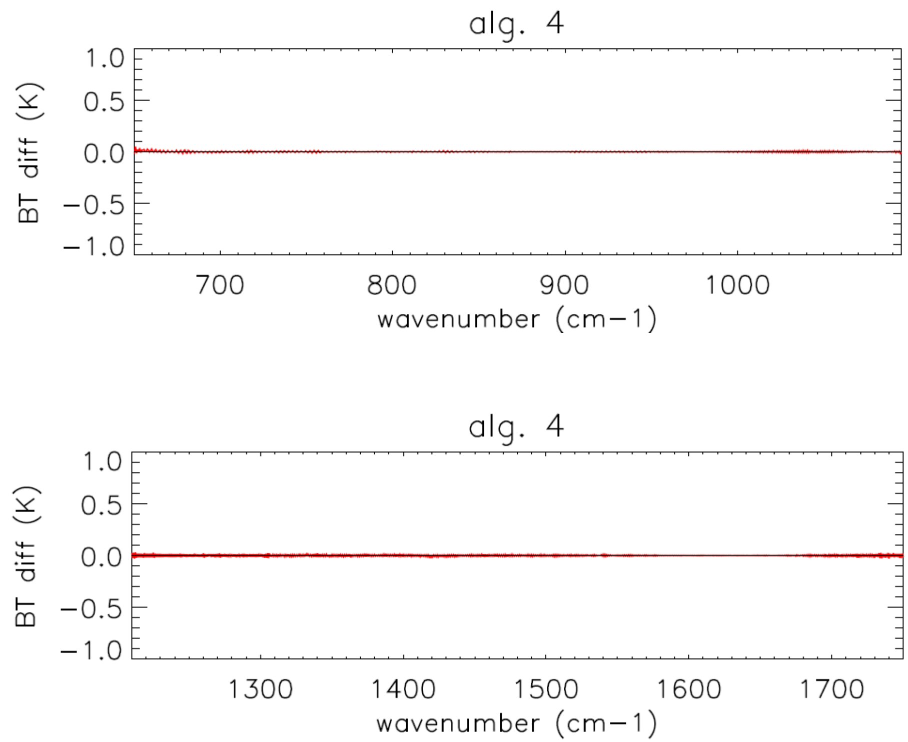

Improving Calibration Equation (1/2)

- Equations differ mainly in how the ratio $\Delta S_1/\Delta S_2$ is filtered before spectral calibration
- The order of spectral calibration components does not have a significant impact
- Algorithm 4 allows the use of a wider PBF *f* (if no aliasing, *f* is not needed)

J1 baseline (algorithm 1):

$$S_{Cal} = SA^{-1}\cdot F\cdot\{f\cdot\frac{\Delta S_1}{\Delta S_2} ICT\}$$

Algorithm 4:

$$S_{Cal} = ICT\cdot\frac{F\cdot SA^{-1}\cdot\{f\cdot\frac{\Delta S_1}{\Delta S_2}|\Delta S_2|\}}{F\cdot SA^{-1}\cdot\{f\cdot|\Delta S_2|\}}$$

Responsivity as a filter

Responsivity removed after spectral calibration

$$\Delta S_1 = FIR^{-1}(S_e - < S_{DS} >)$$

$$\Delta S_2 = FIR^{-1}(< S_{ICT} > - < S_{DS} >)$$

$$= ICT\cdot\frac{F\cdot SA^{-1}\cdot f\cdot\{\frac{\Delta S_1}{Phase(\Delta S_2)}\}}{F\cdot SA^{-1}\cdot f\cdot\{\frac{\Delta S_2}{Phase(\Delta S_2)}\}}$$

Predina's original form

UMBC CCAST:

$$S_{Cal} = ICT\cdot F\cdot SA^{-1}\cdot\{f\cdot\frac{\Delta S_1}{\Delta S_2}\}$$

Improving Calibration Equation (2/2)

- The A4 calibration equation performs spectral calibration on radiometric ratio $\Delta S_1 / \Delta S_2$ filtered with $|\Delta S_2|$ (related to responsivity)

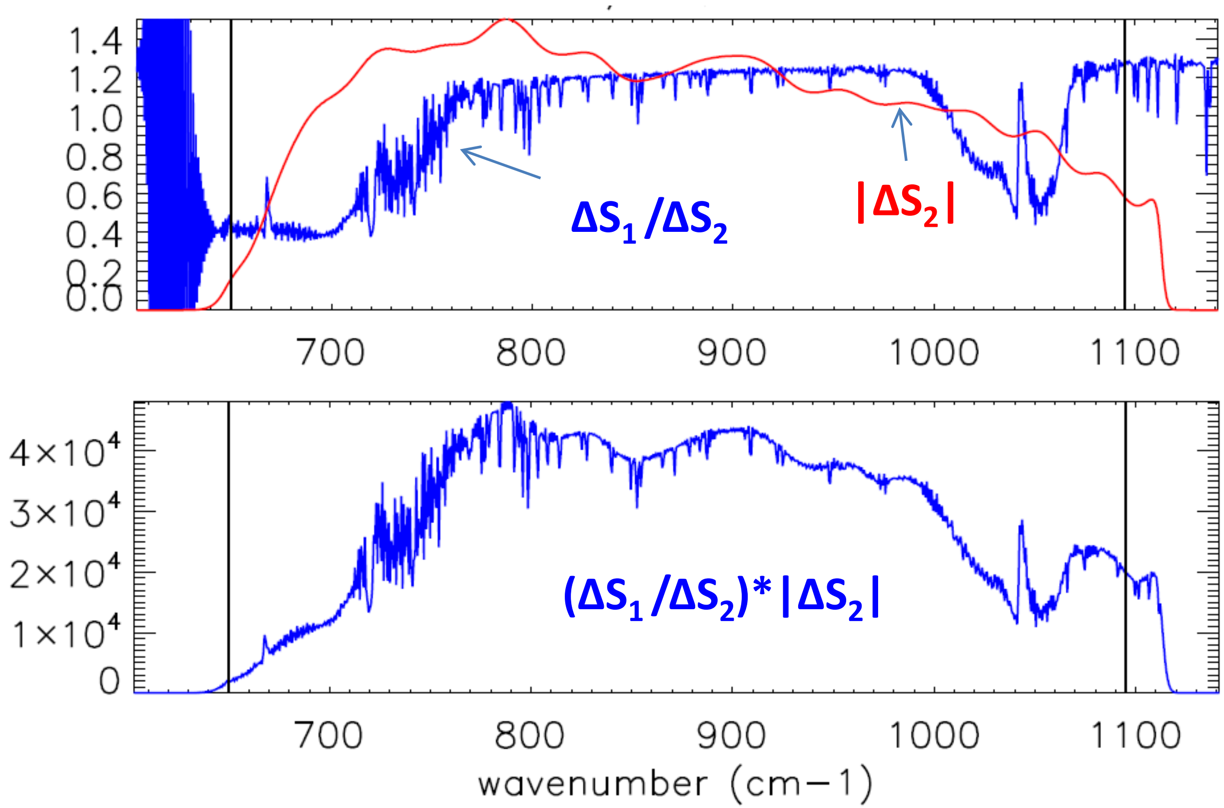

ADL Results

- The following slides show results of obs-cal, sweep direction difference and FOV-to-FOV difference for the LW band (results for MW & SW bands are included in the backup slides

J1 baseline:

$$S_{Cal} = SA^{-1} \cdot F \cdot f \cdot \{\frac{\Delta S_1}{\Delta S_2} ICT\}$$

N_d = 864 (LW), 1050 (MW), 797 (SW)

Algorithm 4:

$$S_{Cal} = ICT \cdot \frac{F \cdot SA^{-1} \cdot f \cdot \{\frac{\Delta S_1}{\Delta S_2} |\Delta S_2|\}}{F \cdot SA^{-1} \cdot f \cdot |\Delta S_2|}$$

N_d = 866 (LW), 1052 (MW), 799 (SW)

Wider f

Observation Compared to LBL Simulation

$BT_{obs} - BT_{lbl}$

Responsivity is used in BT_{lbl} *calculation*

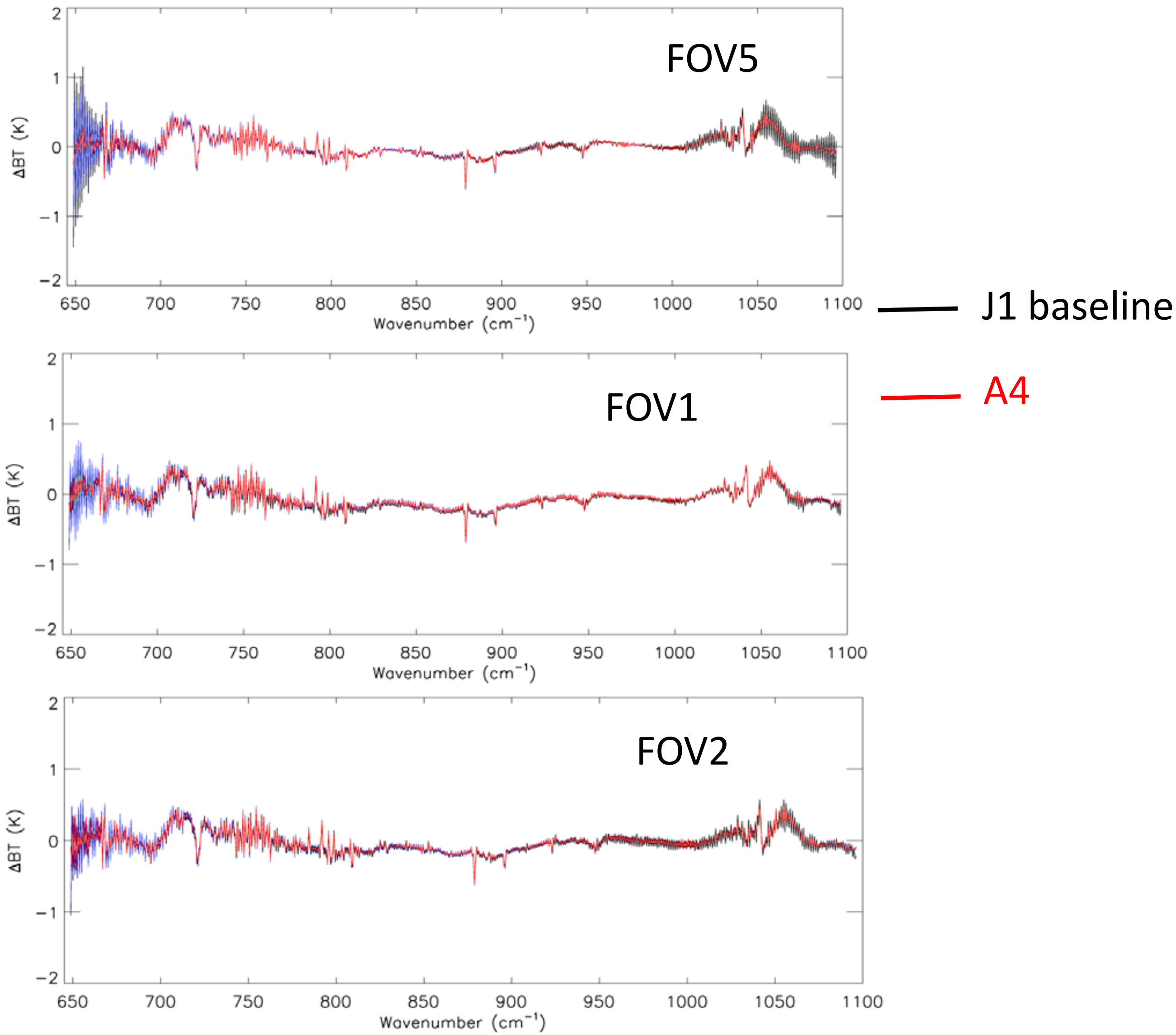

FOV-2-FOV Comparison

J1 baseline

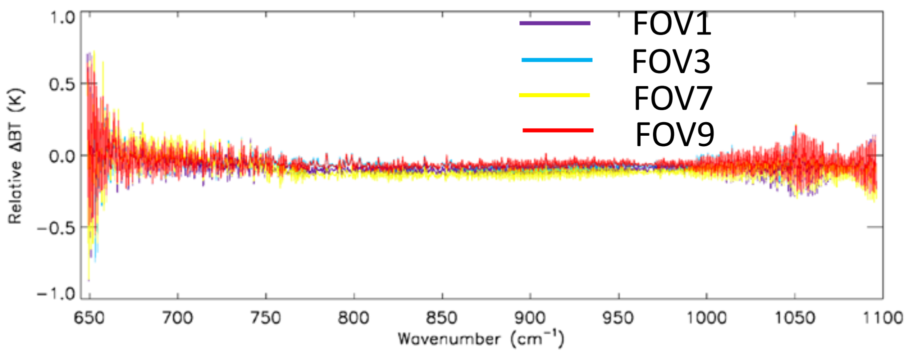

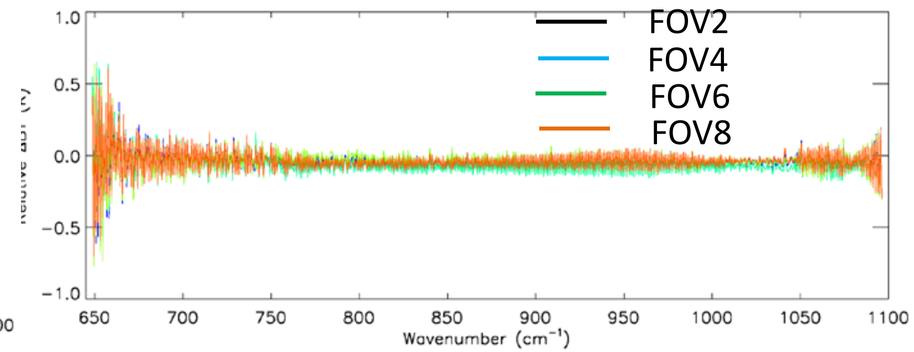

Algorithm 4

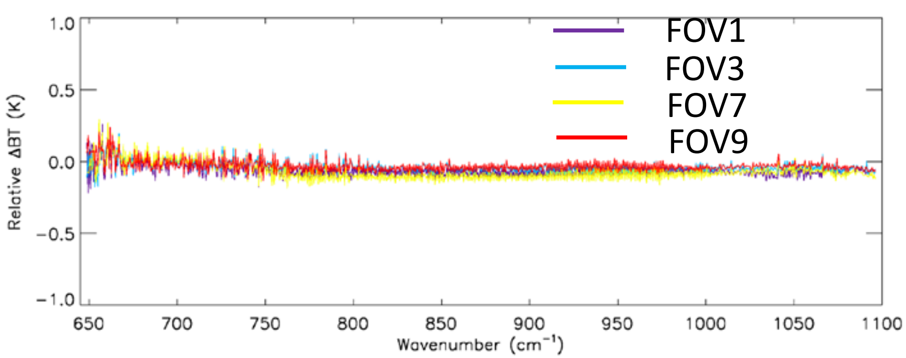

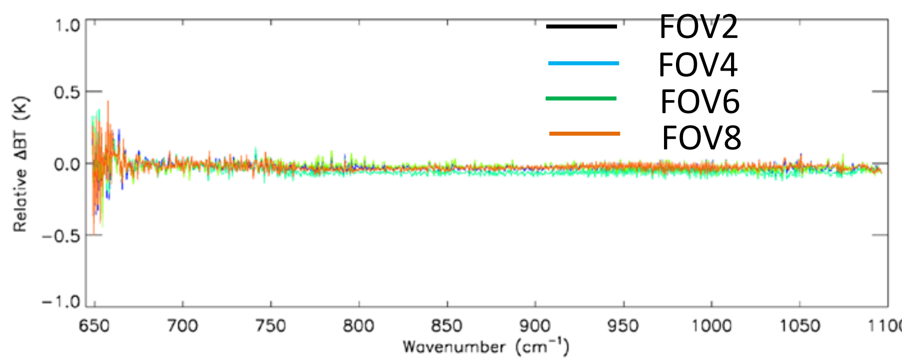

$$(BT_{obs} - BT_{lbl})_{fov\_i} - (BT_{obs} - BT_{lbl})_{fov\_5}$$

Sweep Direction Differences

J1 baseline

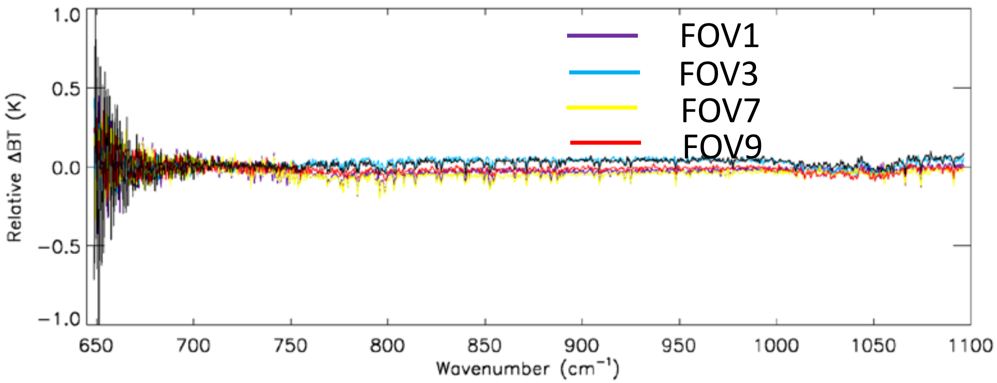

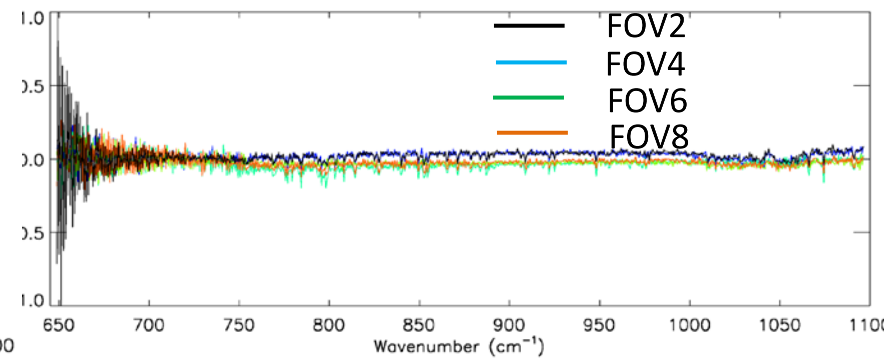

Algorithm 4

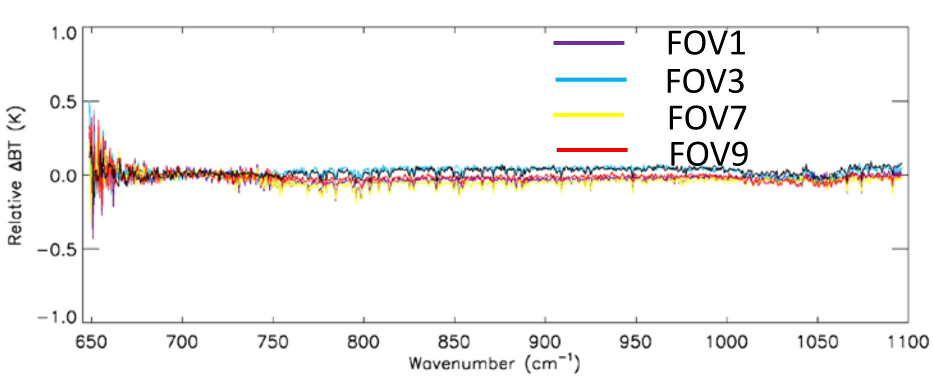

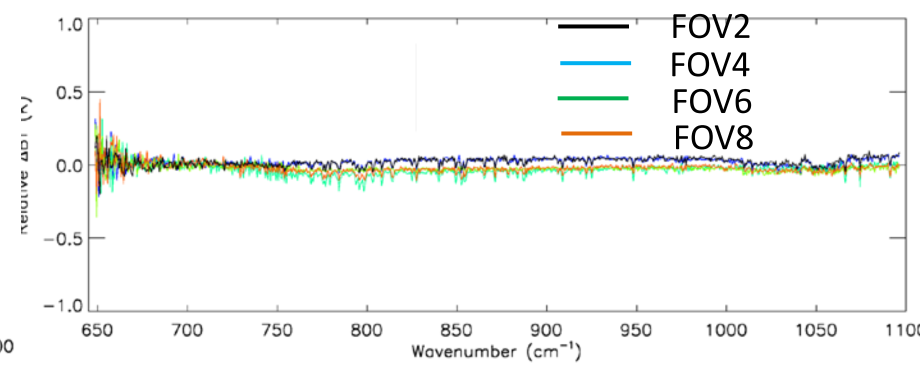

$$(BT_{obs} - BT_{lbl})_{fwd} - (BT_{obs} - BT_{lbl})_{rev}$$

Schedule for Delivery

- The updates described in this presentation will be delivered before the end of 2015 through the DR system
- The updates will also include UMBC calibration equation with flexible parameters to adjust the filter width and position
- The updates will also include the use of band-dependent lunar intrusion thresholds
- The updates can also include the geolocation algorithm correction (need team consensus)

Summary & Future Work

- The baseline J1 CrIS SDR software was delivered with the capability to process FSR SDRs and the backward compatibility for old data
- The proposed updates will significantly reduce radiance ringing artifacts
- The proposed updates will be delivered in December 2015
- Future work:
  - Algorithm evaluation for extended interferograms expected to be available before the end of 2015
  - Post-filter optimization
  - Continuation of evaluations of calibration algorithms
  - Lunar intrusion algorithm improvement
  - Impulse noise spike handling

Backup Slides

Double FFTs vs. Resampling

- Shown here is the equivalence between the double-difference and resampling methods

Start with the raw decimated complex spectrum $\{S_0[k], k = 1, N_d\}$

Double-FFT step 1: divide the raw spectrum by the FIR spectrum as

$$S_1[k] = S_0[k] / FIR[k]$$

Double-FFT step 2: pad zeros to form the spectrum shown below,

$$S_2[k] = \begin{cases} S_1[k - k_0] & k = [k_0, k_0 + N_d - 1] \\ S_1[-k - k_0] & k = [-(k_0 + N_d - 1), -k_0] \\ 0 & otherwise \end{cases}$$

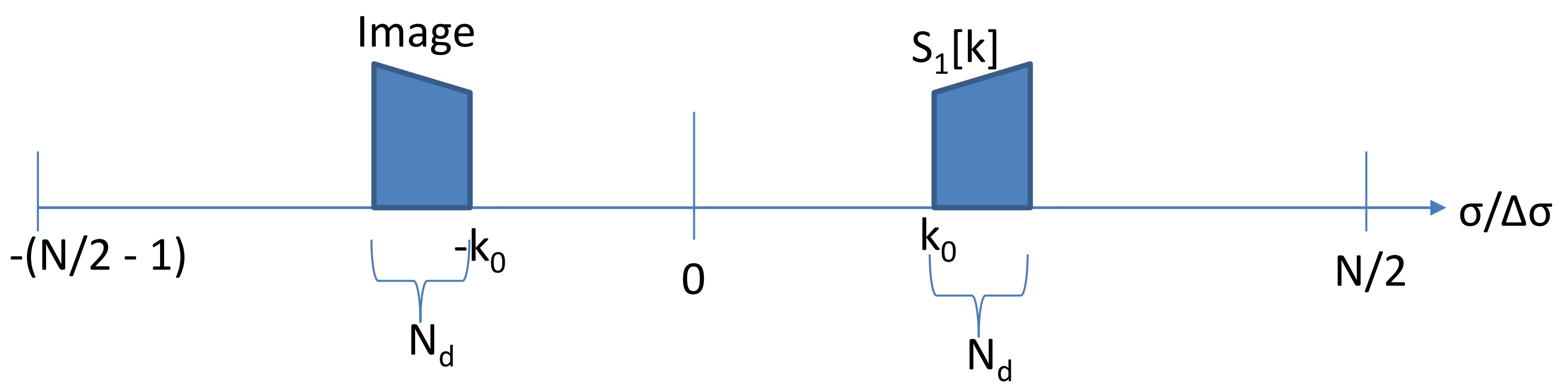

Double FFTs vs. Resampling

Double-FFT step 3: Perform discrete Fourier Transform

$$I_2[n] = \sum_{k=-(N/2-1)}^{N/2} S_2[k] e^{i2\pi nk/N} \Delta\sigma_s \qquad \Delta\sigma_s = \frac{1}{\lambda_s \cdot N_d \cdot DF}$$

Sampling wavelength

Double-FFT step 4: truncate I_2[n] at N_t so that $N_t \lambda_s \approx 1.6\, cm$ and then transform it back to spectrum, which is on the user grid $\Delta\sigma_u = \frac{1}{N_t \Delta x}$:

$$S_3[k] = \sum_{n=-(N_t/2-1)}^{N_t/2} I_2[n] e^{i2\pi nk/N_t} \Delta x \qquad \Delta x = \frac{1}{N \cdot \Delta\sigma_s}$$

Double-FFT step 5: take the in-band channels from S_3[k] to get the final spectrum:

$S = \{S_3[k], k = k_a ... k_b\}$ with a spectral resolution

where $k_a \Delta\sigma_u = \sigma_{k_a}$ and $k_b \Delta\sigma_u = \sigma_{k_b}$ are the starting and ending wavenumbers of the in-band spectrum

Double FFTs vs. Resampling

- Derivation of resampling matrix

Insert the I_2 expression in Double-FFT step 3 into the S_3 expression in Double-FFT step 4:

$$S_3[k] = \sum_{n=-(N_t/2-1)}^{N_t/2} \{ \sum_{k'=-(N/2-1)}^{N/2} S_2[k'] e^{i2\pi n k'/N} \Delta\sigma_s \} e^{-i2\pi n k/N_t} \Delta x$$

$$= \Delta\sigma_s \Delta x \sum_{k'=-(N/2-1)}^{N/2} S_2[k'] \sum_{n=-(N_t/2-1)}^{N_t/2} e^{-i2\pi n(k/N_t - k'/N)}$$

$$= \frac{N_t}{N} \sum_{k'=-(N/2-1)}^{N/2} S_2[k'] \frac{1}{N_t} \sum_{n=-(N_t/2-1)}^{N_t/2} e^{-i2\pi n(k-k'\frac{N_t}{N})/N_t}$$

$$= \frac{N_t}{N} \sum_{k'=-(N/2-1)}^{N/2} S_2[k'] \mathrm{Psinc}(k - k'\frac{N_t}{N}, N_t)$$

$$= \frac{\Delta\sigma_s}{\Delta\sigma_u} \sum_{k'=-(N/2-1)}^{N/2} S_2[k'] \mathrm{Psinc}(\frac{k\Delta\sigma_u - k'\Delta\sigma_s}{\Delta\sigma_u}, N_t)$$

where the relationship $\frac{N_t}{N} = \frac{\Delta\sigma_s}{\Delta\sigma_u}$ is derived from $\Delta\sigma_u = \frac{1}{N_t \Delta x}$ and $\Delta x = \frac{1}{N \cdot \Delta\sigma_s}$

Double FFTs vs. Resampling

- Derivation of resampling matrix

Copy the last equation from previous slide to here:

$$S_3[k] = \frac{\Delta\sigma_s}{\Delta\sigma_u} \sum_{k'=-(N/2-1)}^{N/2} S_2[k']\mathrm{Psinc}\left(\frac{k\Delta\sigma_u - k'\Delta\sigma_s}{\Delta\sigma_u}\right)$$

If we only keep the non-zero terms in the above equation (remember $S_2[k]$ is made of $S_1[k]$ by padding zeros:

$$S_3[k] = \frac{\Delta\sigma_s}{\Delta\sigma_u}\left\{ \sum_{k'=-(k_0+N_d-1)}^{-k_0} S_2[k']\mathrm{Psinc}\left(\frac{k\Delta\sigma_u - k'\Delta\sigma_s}{\Delta\sigma_u}\right) + \sum_{k'=k_0}^{k_0+N_d-1} S_2[k']\mathrm{Psinc}\left(\frac{k\Delta\sigma_u - k'\Delta\sigma_s}{\Delta\sigma_u}\right)\right\}$$

Double FFTs vs. Resampling

- Derivation of resampling matrix

Only the spectrum in the positive frequency domain is what we need; the contribution from the image spectrum (spectrum in the negative frequency domain) is negligible. Thus, the above resampling equation becomes

$$S_3[k] = \frac{\Delta\sigma_s}{\Delta\sigma_u} \sum_{k'=k_0}^{k_0+N_d-1} S_2[k']\mathrm{Psinc}\left(\frac{k\Delta\sigma_u - k'\Delta\sigma_s}{\Delta\sigma_u}, N_t\right)$$

$$= \frac{\Delta\sigma_s}{\Delta\sigma_u} \sum_{k'=0}^{N_d-1} S_1[k']\mathrm{Psinc}\left(\frac{\sigma_{u,k} - \sigma_{s,k'}}{\Delta\sigma_u}, N_t\right)$$

where $\sigma_{u,k} = k\Delta\sigma_u$ and $\sigma_{s,k'} = k'\Delta\sigma_s$ are the wavenumbers on the user and sensor grids

Since N_t is a large number, replace it with N_0 of the undecimated data points will not affect the result of the above equation; thus we have the following final resampling equation matrix:

$$F[k,k'] = \frac{\Delta\sigma_s}{\Delta\sigma_u}\mathrm{Psinc}\left(\frac{\sigma_{u,k} - \sigma_{s,k'}}{\Delta\sigma_u}, N_0\right)$$

Observation Compared to LBL Simulation (MWIR Band)

$BT_{obs} - BT_{lbl}$

Responsivity is used in BT_{lbl} *calculation*

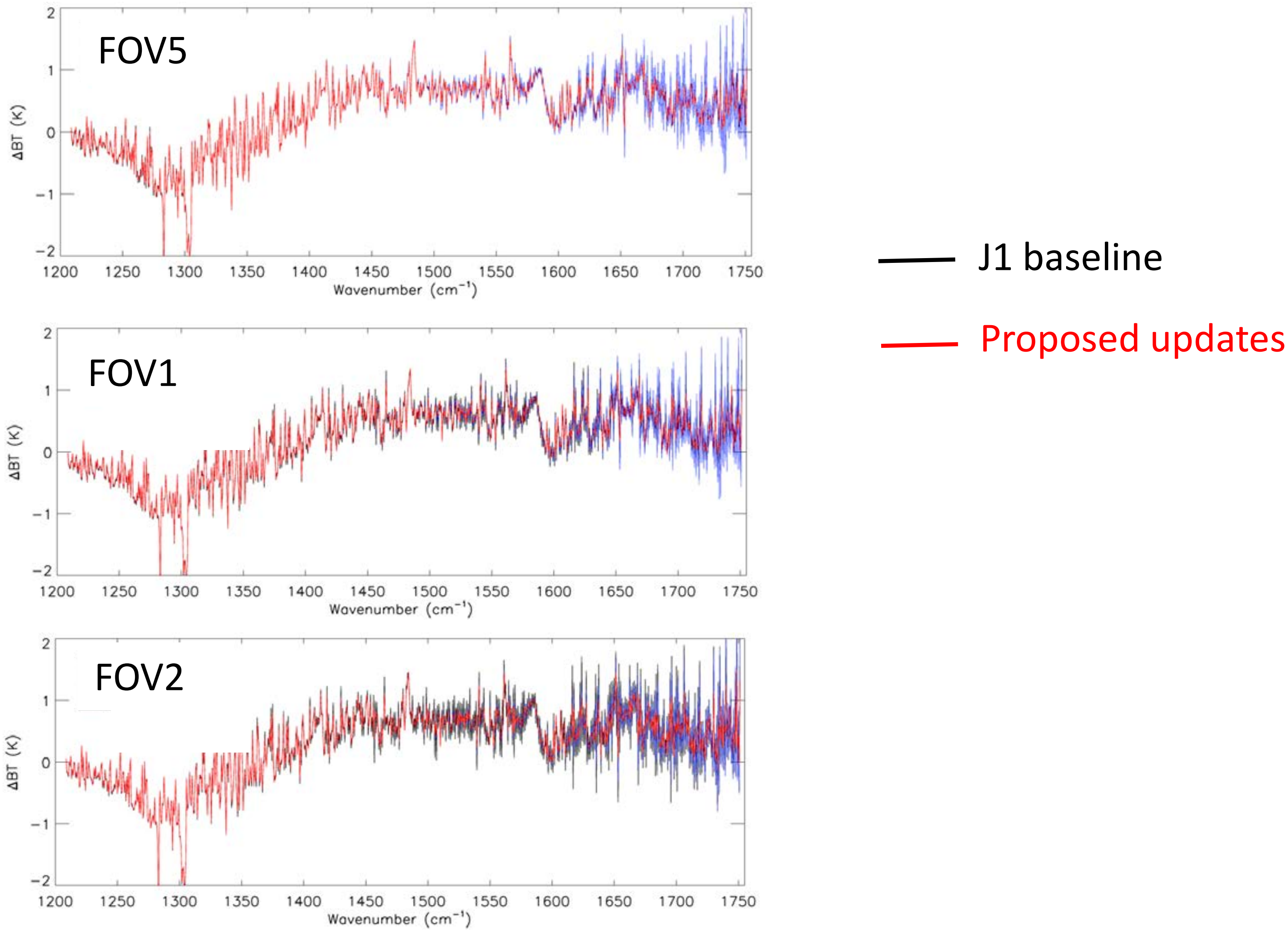

Observation Compared to LBL Simulation (SWIR Band)

$BT_{obs} - BT_{lbl}$

Responsivity is used in BT_{lbl} *calculation*

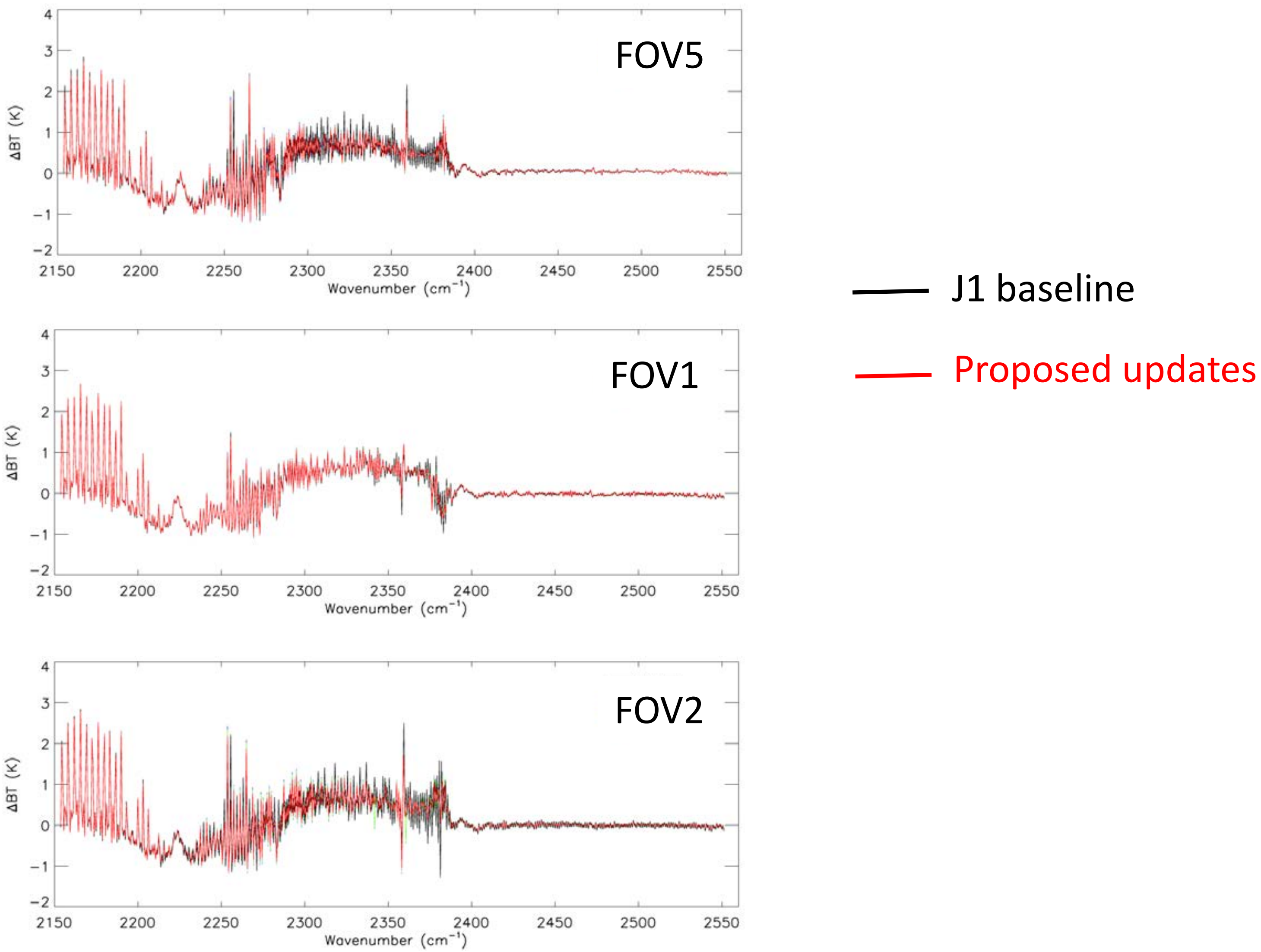

FOV-2-FOV Comparison (MWIR Band)

J1 baseline

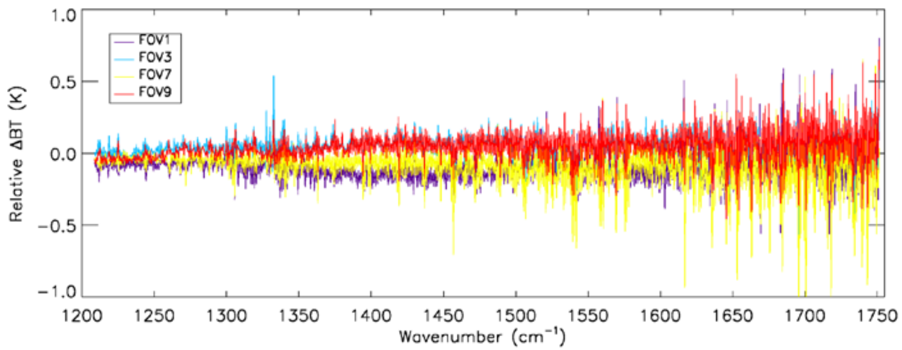

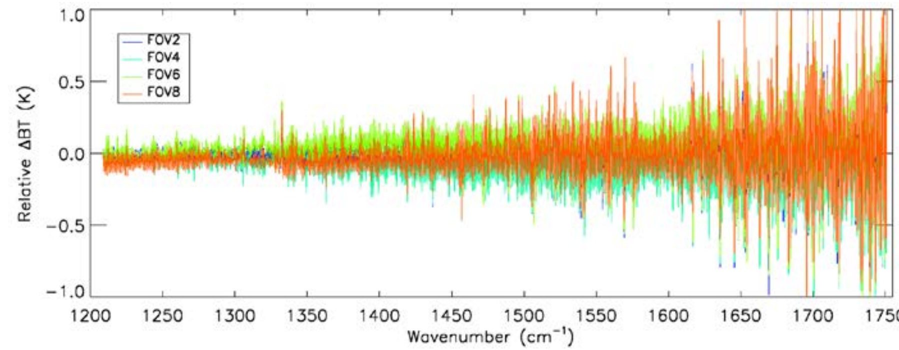

Proposed updates

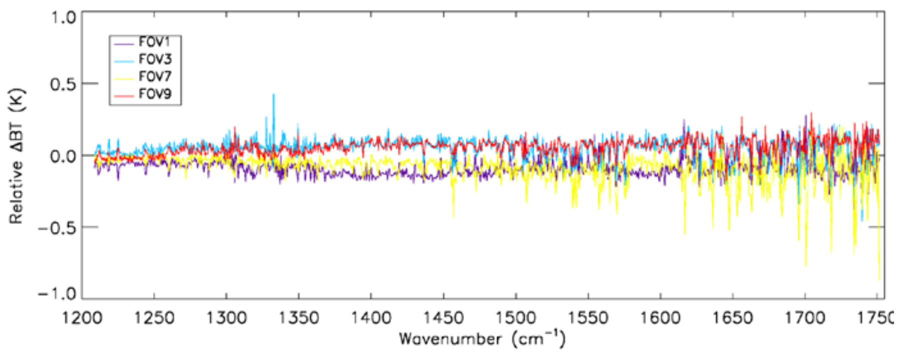

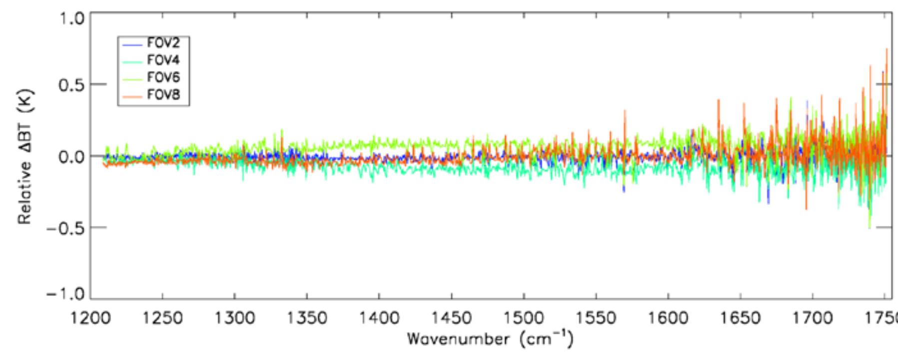

$$(BT_{obs} - BT_{lbl})_{fov\_i} - (BT_{obs} - BT_{lbl})_{fov\_5}$$

FOV-2-FOV Comparison (SWIR Band)

J1 baseline

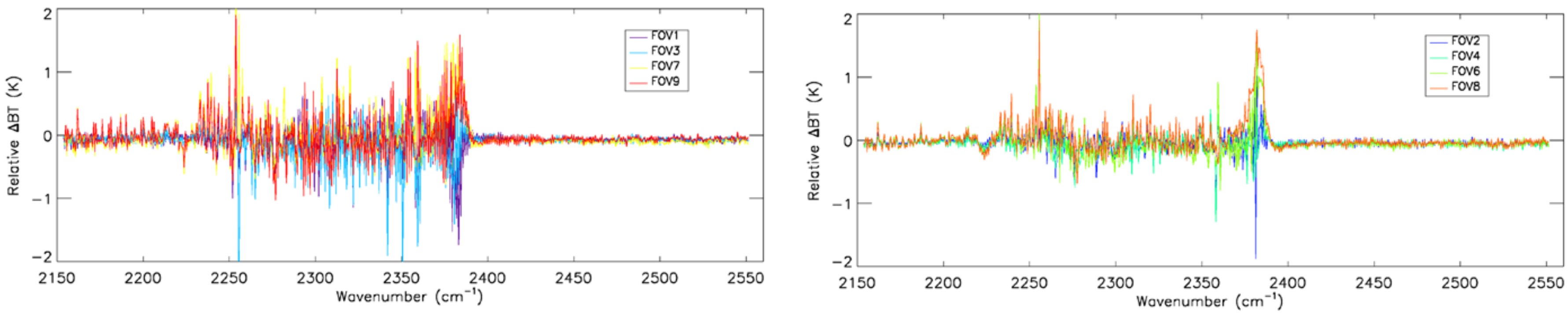

Proposed updates

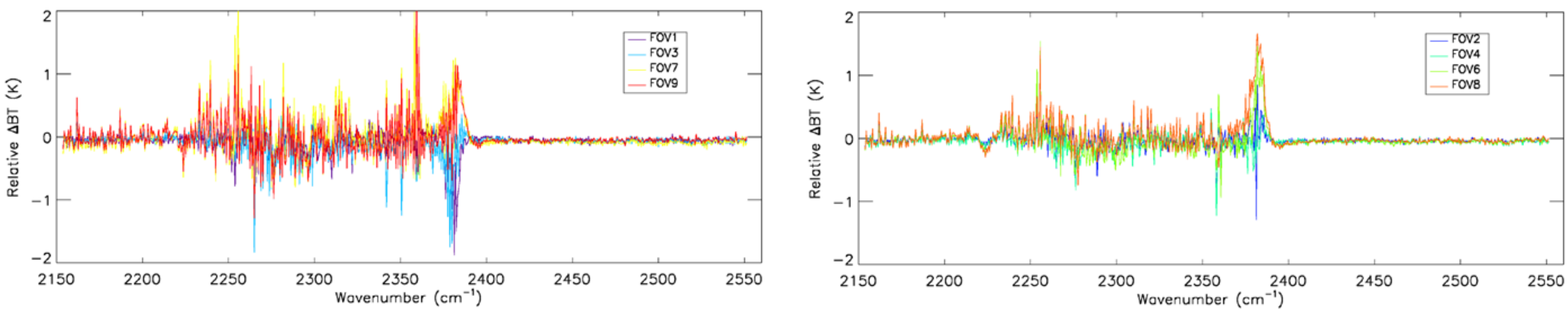

$$(BT_{obs} - BT_{lbl})_{fov\_i} - (BT_{obs} - BT_{lbl})_{fov\_5}$$

Sweep Direction Differences (MWIR Band)

J1 baseline

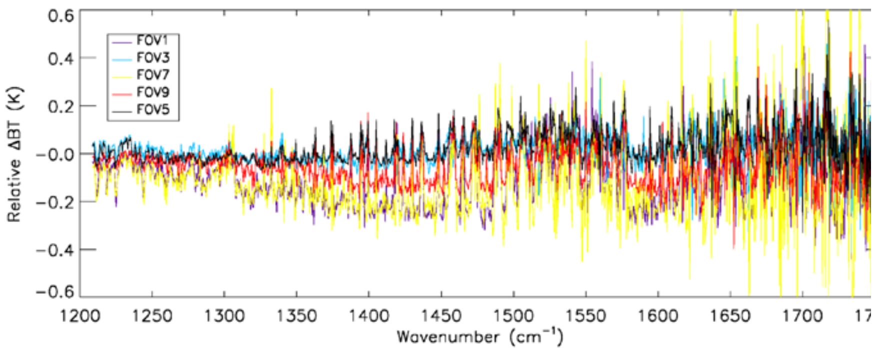

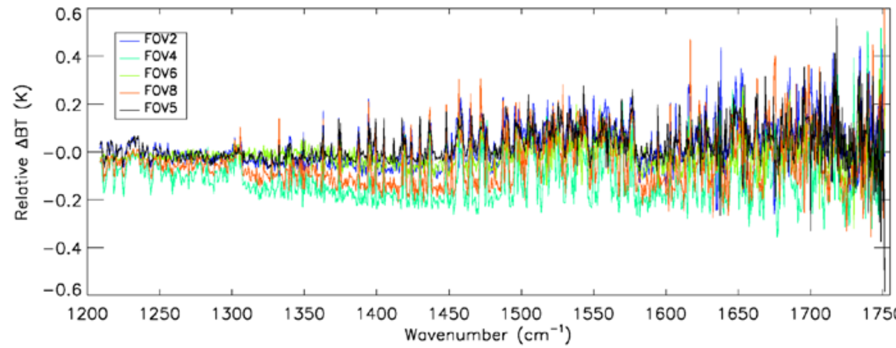

Proposed updates

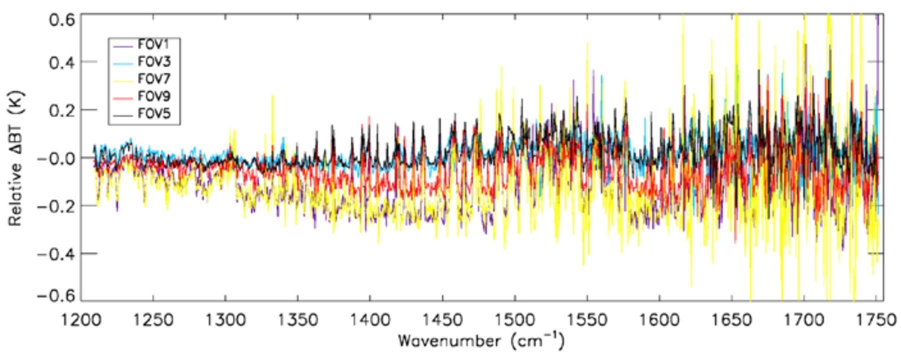

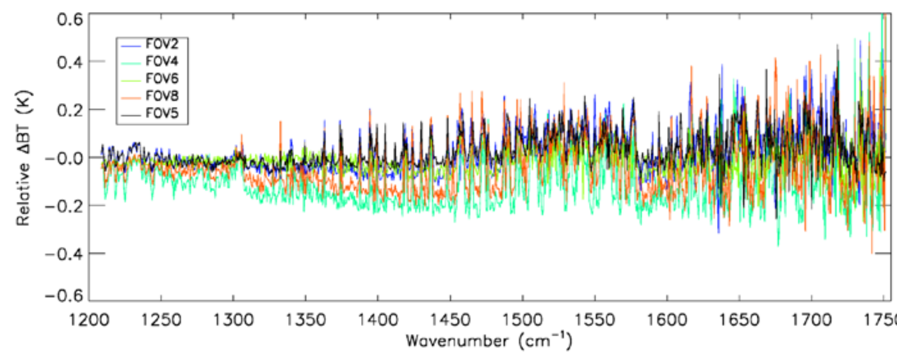

$$(BT_{obs} - BT_{lbl})_{fwd} - (BT_{obs} - BT_{lbl})_{rev}$$

Sweep Direction Differences (SWIR Band)

J1 baseline

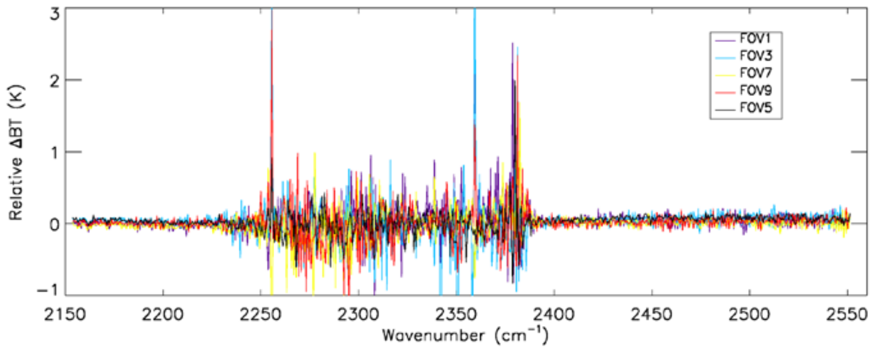

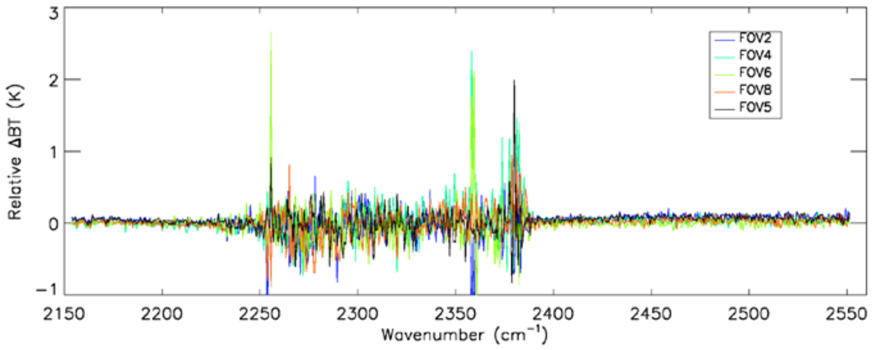

Proposed updates

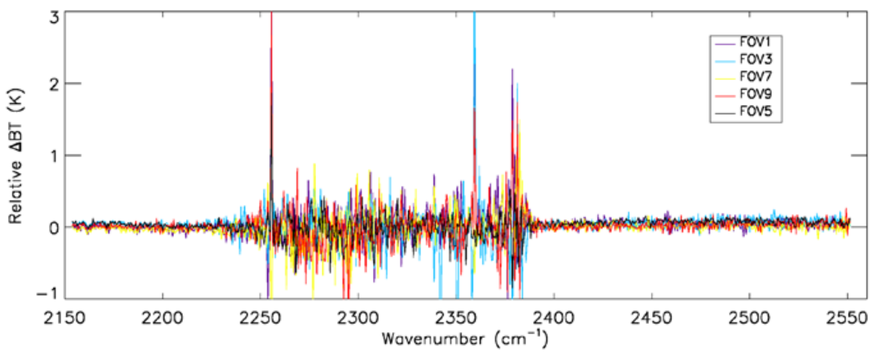

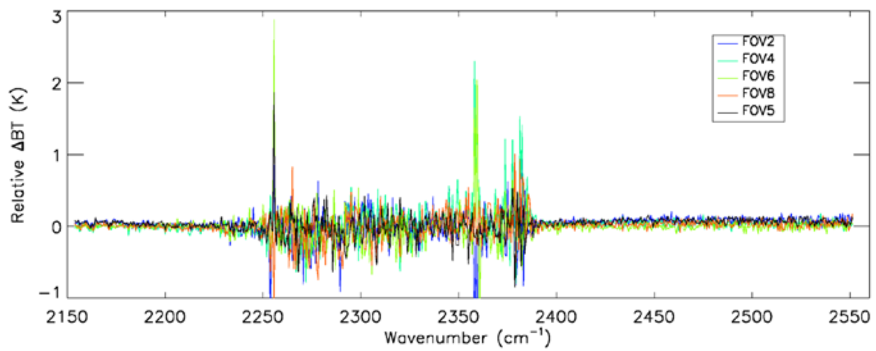

$$(BT_{obs} - BT_{lbl})_{fwd} - (BT_{obs} - BT_{lbl})_{rev}$$